

# Universal Gloss-level Representation for Gloss-free Sign Language Translation and Production

Eui Jun Hwang<sup>1</sup>, Sukmin Cho<sup>1</sup>, Huije Lee<sup>1</sup>,  
Youngwoo Yoon<sup>1,2</sup>, and Jong C. Park<sup>1</sup>

<sup>1</sup> Korea Advanced Institute of Science and Technology (KAIST), Daejeon, Korea  
{ehwa20, nellpic, park}@kaist.ac.kr

<sup>2</sup> Electronics and Telecommunications Research Institute  
youngwoo@etri.re.kr

**Abstract.** Sign language, essential for the deaf and hard-of-hearing, presents unique challenges in translation and production due to its multimodal nature and the inherent ambiguity in mapping sign language motion to spoken language words. Previous methods often rely on gloss annotations, requiring time-intensive labor and specialized expertise in sign language. Gloss-free methods have emerged to address these limitations, but they often depend on external sign language data or dictionaries, failing to completely eliminate the need for gloss annotations. There is a clear demand for a comprehensive approach that can supplant gloss annotations and be utilized for both Sign Language Translation (SLT) and Sign Language Production (SLP). We introduce **Universal Gloss-level Representation (UniGloR)**, a unified and self-supervised solution for both SLT and SLP, trained on multiple datasets including PHOENIX14T, How2Sign, and NIASL2021. Our results demonstrate UniGloR’s effectiveness in the translation and production tasks. We further report an encouraging result for the Sign Language Recognition (SLR) on previously unseen data. Our study suggests that self-supervised learning can be made in a unified manner, paving the way for innovative and practical applications in future research.

## 1 Introduction

Sign language serves as a visual means of communication for the deaf and hard-of-hearing community. In sign language research, there are two main areas: Sign Language Translation (SLT) and Sign Language Production (SLP), both holding a significant social importance. SLT aims to convert sign videos into spoken language, while SLP does the reverse. These processes can be combined in bidirectional SLT systems to facilitate real-time communication between signers and non-signers in practical scenarios [47]. To the best of our knowledge, there are no existing studies that address both SLT and SLP in a unified manner.

Previous studies in SLT [5, 64, 69, 70] and SLP [21, 28, 54, 57, 61] have used glosses, which are written representations of signs. These glosses provide a direct

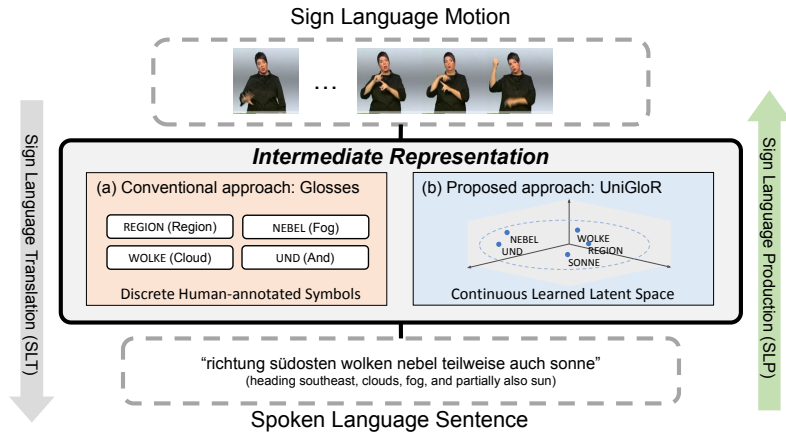


**Fig. 1:** Comparison of the conventional and proposed approaches: (a) incorporating glosses as intermediates, (b) UniGloR, using a learned latent space as intermediates, but not using gloss annotation.

mapping to their corresponding signs, aiding models in learning semantic boundaries within sign language [65]. However, annotating glosses is labor intensive and time-consuming and requires expertise in sign language. Such requirements significantly limit the expansion of sign language datasets [32, 37, 55, 65]. There has been a shift towards gloss-free methods, though they often show lower performance than gloss-based methods. In SLT, several attempts have been made to bridge this performance gap [32, 37, 62], using visual backbone pre-trained on word-level sign language datasets [18, 26, 31]. However, these approaches may not be entirely gloss-free, as they still rely on word-level gloss annotations. In SLP, sign language videos or skeletal poses are often retrieved from pre-defined dictionaries [9, 13, 53]. Although relying on such externally annotated resources could offer interim benefits for both SLT and SLP, they fail to address fundamental issues, limiting adaptability and scalability. Consequently, there is a pressing need for a new representation akin to glosses that serve both SLT and SLP without relying on external annotated resources.

Motivated by these observations, we propose **Universal Gloss-level Representation (UniGloR)**, a unified solution for both SLT and SLP. UniGloR adopts a self-supervised learning approach that can be trained on multiple sign language datasets. Moreover, it eliminates the need for external annotated data and additional adaptation processes, such as fine-tuning, thereby enhancing its applicability. In UniGloR, each sign segment<sup>3</sup> within a pose sequence is uniquely represented, allowing its translation to spoken language sentences and vice versa (Fig. 1). We employ a general framework of autoencoder to process the sign segments and improve the quality of representation by the introduction of Adaptive Pose Weights (APW). APW focuses on subtle yet semantically rich movements in sign language motion, such as facial expressions and hand gestures, ensuring

<sup>3</sup> A sign segment refers to a small fraction of the full sign pose sequence.

proportional attention to each body part based on its movement. Once UniGloR is constructed, the representation is seamlessly integrated into the downstream SLT and SLP tasks.

Experimental results showed superior performance of UniGloR in both SLT and SLP on three datasets: RWTH-PHOENIX-WEATHER-2014T (PHOENIX-14T) [4], How2Sign [14], and NIASL2021 [22]. Furthermore, UniGloR showed its effectiveness in out-of-domain SLR data with KSL-Guide-Word [18]. To summarize, our contributions are threefold:

- We introduce UniGloR, providing a comprehensive solution for both SLT and SLP.
- We introduce APW, to effectively capture the nuances of sign language motion, ensuring proportional attention to each body part for a more precise representation.
- Extensive experiments on diverse datasets, including SLR, demonstrate the effectiveness of our method.

## 2 Related Work

### 2.1 Sign Language Production

Sign Language Production (SLP) aims to translate spoken language or glosses into sign language forms such as videos or pose sequences. Previous works have employed sign language notations such as the glosses [21, 28, 57, 61], HamNoSys [54], and SignWriting [25]. As highlighted in Sec. 1, the challenges associated with the glosses have prompted a shift towards gloss-free methods. These methods broadly fall into two categories: retrieval and generative. Retrieval methods [9, 13, 53] fetch relevant samples from datasets based on textual prompts. By contrast, generative methods can produce entirely new signing sequences by leveraging patterns learned during training. Saunders et al. [51] introduced the Progressive Transformer (PT), an autoregressive model with a counter decoding method. In subsequent studies, they enhanced PT using an adversarial training scheme [50] and a mixture of motion primitives [52]. Meanwhile, Hwang et al. [23] proposed Non-autoregressive Sign Language Production with Gaussian space (NSLP-G), a non-autoregressive SLP model that employs VAE pretrained on the spatial aspects of sign language motion.

### 2.2 Sign Language Translation

Sign Language Translation (SLT) focuses on translating the sign language forms into spoken language sentences. Initially, gloss-based methods [5, 64, 67, 69, 70] were prevalent, using the gloss annotations to effectively align the visual modality and enhance translation quality. Similar to SLP, there has been a shift towards gloss-free methods. Li et al. [32] pioneered it with TSPNet, focusing on temporal semantic structures in the sign videos to enhance feature extraction. Contrastive learning [16, 37] refines representations by adjusting the proximity of positive and

negative pairs. The Gloss Attention mechanism [65] addresses performance gaps resulting from the absence of gloss by focusing its attention on video segments that share similar semantics locally.

A common approach in these gloss-free methods is to pre-train on Sign Language Recognition (SLR) datasets [26, 31], with subsequent task-specific fine-tuning. Our approach diverges from this norm by providing a fixed and enriched gloss-level representation, training on multiple sign language datasets.

### 2.3 Pre-training in Sign Language Research

There has been a growing interest in leveraging pre-training approaches for SLR [26, 31, 33]. Hu et al. [20] introduced SignBERT, a framework that captures the hierarchical context of hand gestures and their temporal dependencies. They adopt a self-supervised approach, masking and reconstructing visual tokens derived from hand poses. Similarly, NC et al. [43] presented Sign2Vec, a model designed to generate semantic vector representations for sign videos, pretrained using Dense Predictive Coding. Zuo et al. [72] introduced VKNet, which consists of two sub-networks to process different frames. Note that we do not categorize continuous SLR models [5, 7, 19, 29, 42, 68, 70] as the gloss-free approach because these models implicitly integrate gloss-related information during training.

Despite the robust pre-training methods, they require fine-tuning when deployed for specific tasks to achieve peak performance. Additionally, their foundational design and pre-training objectives are not inherently aligned with the demands of SLP, which requires the production of continuous sign pose sequences from spoken language sentences. Addressing this gap, our method offers a universal representation for both SLT and SLP, eliminating the need for task-specific fine-tuning and broadening its applicability.

## 3 Universal Gloss-Level Representation

In this section, we introduce **Universal Gloss-Level Representation (UniGloR)**, a unique representation designed for universal application in SLT and SLP. UniGloR leverages an autoencoder to train on multiple datasets, compressing and reconstructing the sign segments for learning meaningful features from raw data. To improve the representation quality, we incorporate Adaptive Pose Weights (APW) which capture detailed motion within the sign segments across spatial and temporal dimensions. We define the problem in Sec. 3.1, present details of the autoencoder in Sec. 3.2, and introduce APW in Sec. 3.3.

### 3.1 Problem Formulation

Given a sign language video  $\mathcal{V} = \{v_t\}_{t=1}^T$ , which consists of  $T$  frames, UniGloR is capable of extracting the representation from the sign segment within  $\mathcal{V}$ . To reduce computational overhead and efficiently process longer sign videos, we use pose keypoints  $X = \{x_t\}_{t=1}^T$ , where each  $x_t \in \mathbb{R}^{V \times C}$ . Here,  $V$  denotes the

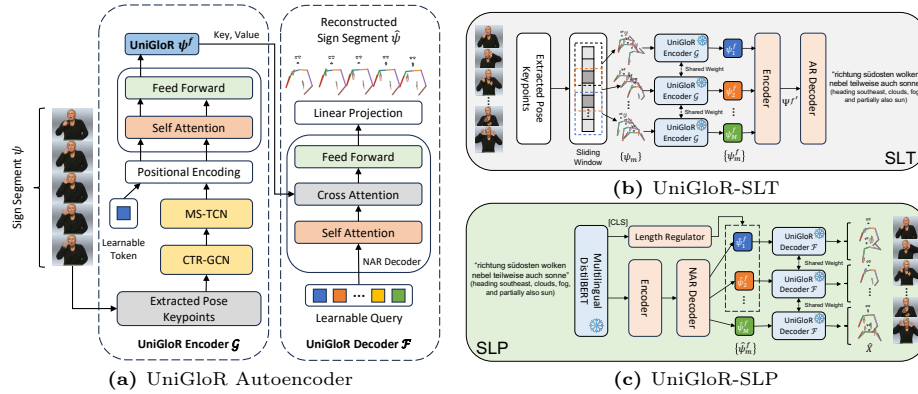


**Fig. 2:** An overview of our UniGloR framework, including its application to downstream tasks. (a) The Transformer encoder-decoder architecture is used to derive a UniGloR  $\psi^f$ . (b) Application to Sign Language Translation (SLT): The frozen UniGloR encoder generates a refined UniGloR sequence with a sliding window approach, subsequently translating them into spoken language sentence. (c) Application to Sign Language Production (SLP): A non-autoregressive (NAR) decoder converts text into a UniGloR sequence, with a length regulation provided by the [CLS] token from a frozen multilingual DistilBERT [49]. The UniGloR sequence is then converted into a sign pose sequence by the frozen UniGloR decoder.

number of vertices, and  $C$  the feature dimension of the skeletal pose data. Within  $X$ , the sign segment is represented as  $\psi = \{x_n\}_{n=1}^N$ , where  $N$  denotes the length of the segment. These sign segments serve as the input for the autoencoder.

### 3.2 UniGloR Autoencoder

As shown in Fig. 2a, we employ an autoencoder based on Transformer encoder-decoder architecture [60]. During training, our framework compresses and reconstructs the sign segments, thereby extracting meaningful features.

The encoder  $\mathcal{G}(\cdot)$  is designed to handle a single sign segment  $\psi$ . The encoding process begins by extracting sign features using CTR-GCN [8] and MS-TCN [39], both of which have been previously utilized in [37]. CTR-GCN is designed for action recognition from skeletal data by dynamically refining the graph topology, while MS-TCN provides a robust framework for the temporal action segmentation. These methods are modified and integrated to extract spatio-temporal features from  $\psi$ . Then, the encoder maps the sign segment into a single latent space, necessitating a temporal dimension pooling. For this purpose, we employ token pooling, drawing inspiration from the [CLS] token in BERT [10] and ViT [12]. We prepend learnable tokens to the extracted features and use only the corresponding outputs for the temporal pooling. The features extracted by CTR-GCN and MS-TCN are then combined with these tokens. The combined input is subsequently summed with sinusoidal positional encodings. We obtain a UniGloR  $\psi^f$  from the first encoder output, while the rest are discarded. The encoding process can be represented as  $\psi^f = \mathcal{G}(\psi)$ , where  $\psi^f \in \mathbb{R}^d$ .

The decoder  $\mathcal{F}(\cdot)$  reconstructs the sign segment  $\psi$  from the given UniGloR  $\psi^f$ . A non-autoregressive decoding is used to address the complexities inherent in an autoregression for continuous data, such as sign pose sequences [21, 23]. We employ a learnable queries  $q$ , motivated from [34], as input to the decoder. These queries interact with self-attention layers and interact with  $\psi^f$ , serving as both key and value, via cross-attention layers. These queries are instrumental in the decoding phase, functioning as initial representations. The decoder then reconstructs the sign segment  $\hat{\psi}$  after a linear projection. The decoding process can be represented as  $\hat{\psi} = \mathcal{F}(q, \psi^f)$ .

### 3.3 Adaptive Pose Weighting

In the fields of pose estimation [56] and generation [71], broad bodily movements are the primary focus. However, it is important to capture subtle movements of hands and facial expressions in sign language. Traditional distance-based loss functions, such as L2 loss [21, 23, 50–52] and L1 loss [57], might not prioritize these finer details, potentially missing nuances in sign language. To address this, we introduce Adaptive Pose Weighting (APW), designed to proportionally adjust the weights based on the variances of movement within each body part, aiming to balance the emphasis between larger and subtle movements. This method ensures that parts with less movement do not become overshadowed by those with more significant movement.

The first step involves splitting the keypoints into three distinct categories: body, face, and hands, represented as  $X = [X^b; X^f; X^h]$ . We then calculate the spatio-temporal variances for each category across all frames, denoted as  $\sigma_b^2, \sigma_f^2$ , and  $\sigma_h^2$  for the body, face, and hands, respectively. For the hands, we measure residual movement  $\sigma_{rh}^2$  by calculating the positional difference between each hand and its corresponding wrists, represented as  $X^{rh} = X^h - X^{wrist}$ . For the face, we normalize the keypoints  $X^{nf}$  by calculating their spatial centroids  $\mu_f \in \mathbb{R}^{T \times 1}$  and adjusting the face keypoints accordingly, represented as  $X^{nf} = X^f - \mu_f$ . To assign adaptive weights, we use these variances to measure the dynamic importance of each category. The weight for each category is calculated as:

$$w^p = 1 - \frac{\sigma_p^2 + \sigma_b^2}{\sum \sigma^2}, \quad p \in \{b, nf, rh\}, \quad (1)$$

where  $p$  represents the particular part. Here,  $\sigma_b^2$ , the variance of the body part, serves as the baseline for adjusting the weights of other parts. This ensures that both the larger body movement and the subtler movements are equally emphasized over the entire sequence of frames. Then, the weights for each frame  $t$  are represented as  $W_t = [W_t^b; W_t^{nf}; W_t^{rh}]$ , where  $W_t^p = \{w_1^p, w_2^p, \dots, w_{N(p)}^p\}$ , with  $N(p)$  being the number of keypoints in the categories. The resulting total loss is defined as:

$$\mathcal{L} = \sum_{t=1}^N W_t \left\| \psi_t - \hat{\psi}_t \right\|_2^2. \quad (2)$$

## 4 Application of UniGloR

In this section, we describe how a UniGloR sequence is applied in downstream tasks such as Sign Language Translation (SLT) and Sign Language Production (SLP). As shown in Figs. 2b and 2c, we utilize the Transformer to bridge different modalities between the UniGloR sequence and spoken language sentence.

### 4.1 UniGloR-SLT

Given an extracted sign pose sequence  $X$ , the goal of SLT is to generate a spoken language sentence  $Y = \{y_u\}_{u=1}^U$  consisting of  $U$  words. This translation process can be represented as a conditional probability of  $P(Y|X)$ . As shown in Fig. 2b,  $X$  is segmented into  $\Psi = \{\psi_m\}_{m=1}^M$ , where  $M$  denotes the total number of the sign segments. The UniGloR sequence can then be expressed as  $\Psi^f = \{\psi_m^f\}_{m=1}^M$ , where each  $\psi_m^f \in \mathbb{R}^d$ . The translation from  $X$  to  $Y$  considers the joint probability of  $Y$  and  $\Psi^f$ , represented as  $P(Y, \Psi^f|X) = P(Y|\Psi^f)P(\Psi^f|X)$ .

For  $P(\Psi^f|X)$ , we use the frozen encoder  $\mathcal{G}$  (Sec. 3.2) to generate the sequence  $\Psi^f$ . However, accurately determining the boundaries of the sign segments is challenging. To overcome this challenge, we adopt a sliding window approach to define the sign segments, mostly following [32]. We set a window size  $w \in \mathbb{N}$  and an overlap  $o \in \mathbb{N}$ , with a stride  $s$  determined as  $w - o$ . This generates  $\Psi = \{\psi_{ks:ks+w} \mid 0 \leq k < \lfloor \frac{T}{w} \rfloor\}$ , where  $\psi_{ks:ks+w}$  includes indices from  $ks$  to  $ks + w$ , capturing the span from the start to the end of each window. The final output from this procedure is given as  $\Psi^f = \{\mathcal{G}(\psi_m)\}_{m=1}^M$ .

Subsequently, the sequence  $\Psi^f$  is encoded with the Transformer encoder, generating  $\Psi^{f'}$  that includes attention-enriched features. This representation is then passed to an autoregressive decoder, which iteratively constructs the spoken language sentence  $Y$  word by word. At each decoding step, the model calculates the conditional probability  $P(y_i|y_{<i}, \Psi^{f'})$  for the next word  $y_i$ , based on the preceding words  $y_{<i}$  and the encoded sequence  $\Psi^{f'}$ .

The training objective is to minimize a cross-entropy loss, given by:

$$\mathcal{L} = - \sum_{i=1}^U \log P(y_i|y_{<i}, \Psi^{f'}). \quad (3)$$

### 4.2 UniGloR-SLP

The process of SLP can be represented by the conditional probability  $P(X|Y)$ , which is the inverse of SLT (Sec. 4.1). Inspired by [46], we formulate the conditional probability for SLP as  $P(X, \Psi^f, L|Y) = P(X|\Psi^f, L, Y)P(\Psi^f|Y)P(L|Y)$ , where  $P(X|\Psi^f, Y)$  handled by the frozen UniGloR decoder,  $P(\Psi^f|Y)$  by the non-autoregressive Transformer, and  $P(L|Y)$  by a length regulator.

Specifically, as shown in Fig. 2c,  $Y$  is initially processed through the multi-lingual DistilBERT [49] to extract enriched linguistic features. The [CLS] token from this embedding is used to determine the length for the UniGloR sequence. It

does so through the length regulator comprised a several linear layers, addressing the specific needs of non-autoregressive decoding. The remaining tokens are then fed into the Transformer encoder-decoder architecture with non-autoregressive decoding, similar to [23], to generate the sequence  $\hat{\Psi}^f$ . We use fixed-length learnable queries as input for the decoder. Finally, the decoder output, regulated in length, is converted into a sign pose sequence using the frozen UniGloR decoder.

The training objective is to minimize two distinct losses: one for the generated UniGloR sequence and another for the generated length. The first loss, employing L2 loss, measures the difference between  $\Psi^f$ , which is encoded from ground-truth sign poses by the frozen UniGloR encoder, and the generated  $\hat{\Psi}^f$ . It can be represented as:

$$\mathcal{L}_{\text{seq}} = \sum_{i=1}^M \left\| \psi_i^f - \hat{\psi}_i^f \right\|_2^2, \quad (4)$$

where  $M$  denotes the length of the UniGloR sequence. The second loss can be represented as:

$$\mathcal{L}_{\text{len}} = - \sum_{i=1}^C l_i \cdot \log(p_i) \quad (5)$$

where  $C$  denotes the number of possible lengths of the UniGloR sequence, which can be considered discrete classes as in many Natural Language Processing (NLP) tasks [2, 11, 30, 38],  $l_i$  the actual length of the UniGloR sequence, and  $p_i$  the predicted probability of the target length.

The resulting total loss is defined as a summation of  $\mathcal{L}_{\text{seq}}$  and  $\mathcal{L}_{\text{len}}$  as:  $\mathcal{L} = \mathcal{L}_{\text{seq}} + \mathcal{L}_{\text{len}}$ . Finally,  $\hat{\Psi}^f$  is fed to the decoder  $\mathcal{F}$  as described in Sec. 3.2, resulting in the sign pose sequence can be represented as  $\hat{X} = \{\mathcal{F}(\psi_m)\}_{m=1}^M$ .

## 5 Experiments

### 5.1 Datasets

We evaluated our method using three different sign language datasets: RWTH-PHOENIX-WEATHER-2014T (PHOENIX14T) [4], How2Sign [14] and NIASL20-21 [22]. PHOENIX14T features German Sign Language (DGS) from weather forecasts; How2Sign, American Sign Language (ASL) from instructional videos; and NIASL2021, Korean Sign Language (KSL) from emergency alerts and weather forecasts. More details of each dataset can be found in Tab. 1. For PHOENIX14T, where keypoints are not provided, we used OpenPose [6] and skeleton correction model [66], following [23, 51]. Additionally, to assess our method’s adaptability to out-of-domain (unseen) data, we used KSL-Guide-Word [18], covering the transportation and direction domain. This dataset features 3,000 isolated words performed by 20 native signers.



**Table 1:** Statistics of Sign Language Datasets. NoF means the number of frames. We also present the number of named entities (NEs) per sentence for each dataset, identified using spaCy (<https://spacy.io/>).

Dataset	Lang	Vocab	Train / Valid / Test	Avg NoF	#NEs/sent	#Words/sent	#NEs/words(%)	Gloss
PHOENIX14T [4]	DGS	3K	7,096 / 519 / 642	116	0.74	13.77	5.43%	✓
How2Sign [14]	ASL	16K	31,128 / 1,741 / 2,322	173	0.12	20.33	0.61%	✗
NIASL2021 [22]	KSL	8K	160,644 / 10,079 / 9,989	466	2.31	12.30	18.85%	✓

## 5.2 Metrics

We used BLEU [44] and ROUGE-L [36] as evaluation metrics [4] for SLT. BLEU-4 combines precision scores for 1, 2, 3, and 4-grams, measuring the linguistic accuracy of our translations. ROUGE-L focuses on the longest shared subsequences between the predicted and reference translations, calculating the F1 score for text similarity. Higher scores in both metrics indicate better performance. In SLP, we used Back-Translation (BT) [51] to measure BLEU scores, translating the produced sign pose sequence back into spoken language for comparison with the original text. As a back-translation model, we trained Joint-SLT [5] on PHOENIX14T, How2Sign, and NIASL2021, respectively, following [21, 23, 24, 51, 57]. Additionally, we measured Mean Per Joint Position Error (MPJPE), a metric commonly used in human motion prediction tasks [3, 17, 35].

## 5.3 Implementation and Training Details

For pre-training UniGloR, we used an input size of 15 frames, each representing keypoints in an abstract form to focus on essential elements. It can be represented as  $15 \times 73 \times 2$ , where 73 represents the number of joints and 2 refers to the  $x$  and  $y$  coordinates. The segment size was decided based on the findings of [63], indicating that a single sign is optimally captured within 15 frames. For data augmentation purposes, we randomly selected the sign segments within the sign pose sequence during training. For the temporal domain, we applied random masking in a ratio of 10%. For the spatial domain, Gaussian noise [23, 24, 51] was introduced, with its value linearly increased from 0.01 to 0.1.

Our UniGloR autoencoder and downstream models, including SLR, are based on the vanilla Transformer encoder-decoder architecture [60]. Our pre and subsequent training configurations mostly follow [5]. We used AdamW [40] optimizer with a batch size of 64. The autoencoder was trained across PHOENIX14T, How2Sign, and NIASL2021. For SLT, we set the window size  $w$  and the overlap size  $o$  to 15 and 8, respectively. For SLP, we used a variant of DistilBERT<sup>4</sup> from HuggingFace. Further details are provided in the supplementary material.

## 5.4 Comparison with State-of-the-art

In SLT, we compared our method against four baselines: CTR-GCN [8], MS-TCN [39], Joint-SLT [5], and ConSLT [16]. To accommodate the different input modalities (RGB vs. keypoints), we modified most baselines to accept keypoints

<sup>4</sup> <https://huggingface.co/M-CLIP/M-BERT-Distil-40>

**Table 2:** Performance comparison on PHOENIX14T, How2Sign, and NIASL2021. B@N and R@L denote the BLEU-N, and ROUGE-L scores, respectively. We reproduced most baselines due to the different modality of nature (RGB vs. keypoints).  $\star$  denotes modification to accept keypoints as input.  $\dagger$  denotes results reproduced under the gloss-free setting.  $\ddagger$  denotes results reproduced without ground-truth. The best results are highlighted in bold.

SLT Models	B@1	B@2	B@3	B@4	R@L	SLP Models	B@1	B@2	B@3	B@4	R@L	MPJPE $\downarrow$
RWTH-PHOENIX-WEATHER-2014T						RWTH-PHOENIX-WEATHER-2014T						
CTR-GCN [8]	22.41	14.57	10.82	8.66	22.10	PT $\ddagger$ [51]	12.07	5.94	4.04	3.08	11.06	0.602
CTR-GCN [8] + MS-TCN [39]	22.10	14.51	10.70	8.62	21.82	NSLP-G [23]	19.10	12.10	8.87	6.97	18.62	0.335
Joint-SLT $^{\star}$ [5]	21.31	14.17	10.05	8.12	22.56							
ConSLT $^{\star}$ [16]	21.09	13.93	10.48	8.49	21.81							
UniGloR-SLT (Ours)	<b>26.68</b>	<b>18.22</b>	<b>13.73</b>	<b>11.01</b>	<b>27.03</b>	UniGloR-SLP (Ours)	<b>29.60</b>	<b>21.25</b>	<b>16.48</b>	<b>13.44</b>	<b>31.38</b>	<b>0.183</b>
How2Sign						How2Sign						
CTR-GCN [8]	13.81	5.51	2.42	0.88	10.81	PT $\ddagger$ [51]	11.88	4.50	1.75	0.42	9.76	0.466
CTR-GCN [8] + MS-TCN [39]	13.33	5.70	2.61	1.00	11.03	NSLP-G [23]	9.73	3.67	1.53	0.48	10.18	0.427
Joint-SLT $^{\star}$ [5]	11.11	4.41	1.98	0.78	10.61							
ConSLT $^{\star}$ [16]	12.06	4.75	1.92	0.84	9.72							
UniGloR-SLT (Ours)	<b>14.26</b>	<b>5.99</b>	<b>2.96</b>	<b>1.47</b>	<b>11.05</b>	UniGloR-SLP (Ours)	<b>12.69</b>	<b>5.12</b>	<b>2.36</b>	<b>1.06</b>	<b>10.93</b>	<b>0.169</b>
NIASL2021						NIASL2021						
CTR-GCN [8]	46.15	36.43	29.70	24.97	45.96	PT $\ddagger$ [51]	0.87	0.42	0.22	0.10	0.99	0.521
CTR-GCN [8] + MS-TCN [39]	46.74	37.09	30.39	25.50	46.53	NSLP-G [23]	3.17	1.04	0.39	0.13	3.22	0.464
Joint-SLT $^{\star}$ [5]	45.61	36.08	29.58	24.84	45.45							
ConSLT $^{\star}$ [16]	46.50	37.00	30.51	25.78	46.24							
UniGloR-SLT (Ours)	<b>49.49</b>	<b>39.68</b>	<b>32.80</b>	<b>27.69</b>	<b>48.81</b>	UniGloR-SLP (Ours)	<b>5.41</b>	<b>2.48</b>	<b>1.03</b>	<b>0.42</b>	<b>6.02</b>	<b>0.448</b>

(a) Translation performance

(b) Production performance

**Table 3:** Performance comparison on PHOENIX14T and NIASL2021 with gloss-based methods. We exclude How2Sign due to the absence of glosses.

SLT Models	B@1	B@2	B@3	B@4	R@L	SLP Models	B@1	B@2	B@3	B@4	R@L	MPJPE $\downarrow$
RWTH-PHOENIX-WEATHER-2014T						RWTH-PHOENIX-WEATHER-2014T						
Joint-SLT $^{\star}$ [5]	24.88	15.98	11.66	9.28	24.76	PT $\ddagger$ [51]	14.84	8.00	5.49	4.19	12.83	0.590
SLTUNET $^{\star}$ [67]	25.34	17.24	13.02	10.63	25.56	NSLP-G [23]	18.25	11.06	7.86	6.14	17.71	0.332
UniGloR-SLT (Ours)	<b>26.68</b>	<b>18.22</b>	<b>13.73</b>	<b>11.01</b>	<b>27.03</b>	UniGloR-SLP (Ours)	<b>29.60</b>	<b>21.25</b>	<b>16.48</b>	<b>13.44</b>	<b>31.38</b>	<b>0.183</b>
NIASL2021						NIASL2021						
Joint-SLT $^{\star}$ [5]	<b>53.27</b>	<b>43.92</b>	<b>37.22</b>	<b>32.16</b>	<b>52.91</b>	PT $\ddagger$ [51]	1.53	0.54	0.25	0.07	1.85	0.407
SLTUNET $^{\star}$ [67]	52.36	43.03	36.39	31.39	52.07	NSLP-G [23]	4.17	1.82	0.89	0.36	4.26	0.453
UniGloR-SLT (Ours)	49.49	39.68	32.80	27.69	48.81	UniGloR-SLP (Ours)	<b>5.41</b>	<b>2.48</b>	<b>1.03</b>	<b>0.42</b>	<b>6.02</b>	<b>0.448</b>

(a) Translation Performance

(b) Production Performance

as input and reproduced results under a gloss-free setting. Specifically, we report evaluation results of Joint-SLT with and without CTC loss, ConSLT in its “sign2text” setting and SLTUNET without the use of an external data. This modification reveals a performance gap similar to that observed in modified versions of Joint-SLT when comparing RGB and keypoint modalities [21, 23, 24, 57], showing that the reproduction is acceptable.

As shown in Tab. 2a, our method consistently outperformed the baselines across PHOENIX14T, How2Sign, and NIASL2021. On PHOENIX14T, our method achieved a BLEU-4 of 11.01 over the next best score of 8.66 and a ROUGE-L of 27.03 compared to 22.56. On NIASL2021, we achieved a BLEU-4 of 27.69 and a ROUGE-L of 48.81. However, on How2Sign, with a BLEU-4 of 1.47 and ROUGE-L of 11.05, the performance was lower than on the other datasets while our method still showed better performance than the baselines. This can be attributed to the broader domain range of the dataset and its substantially large unique word count, about five times that of PHOENIX14T (Tab. 1). More-

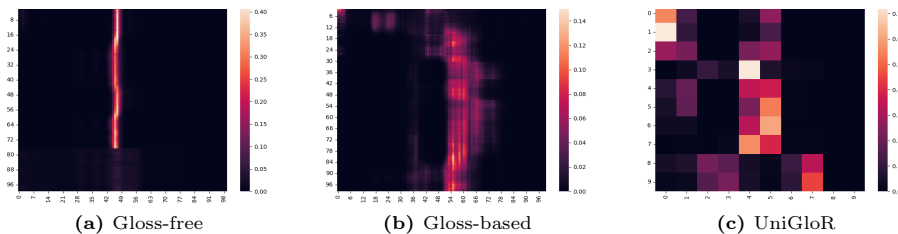


**Fig. 3:** Visualization of the attention maps in the shallow encoder layer of gloss-free, gloss-based, and UniGloR-SLT models, illustrating how each model focuses on different aspects of the input data. The X and Y axes represent keys and queries, respectively.

over, How2Sign contains far fewer samples compared to NIASL2021, showing the dataset’s complexity and the challenges it poses for translation.

Next, we compared our SLP method with existing methods, PT [51] and NSLP-G [23]. PT was modified to exclude the use of additional ground-truth data, as recommended by [21, 24, 57], to ensure a fair comparison. For NSLP-G, we used the fine-tuning option during training. As shown in Tab. 2b, our method significantly outperformed NSLP-G on PHOENIX14T, improving a BLEU-4 by 6.9 and reducing a MPJPE by 0.15. On How2Sign, it achieved a BLEU-4 of 1.06 and a MPJPE of 0.169, demonstrating consistent superiority. While our method achieved the best performance on NIASL2021, the scores were not comparable to the ones on the other datasets due to the challenge of generating longer sequences (Tab. 1). A more detailed analysis of the sequence length of each dataset is available in the supplementary material.

We also compared our method to gloss-based methods. Note that, in SLT, the term “gloss-based” means that the models are gloss-supervised; in SLP, it refers to gloss-to-pose direction. As shown in Tab. 3a, on PHOENIX14T, our method achieved a BLEU-4 of 11.01, outperforming SLTUNET by 0.38 and Joint-SLT by 1.73. However, the gloss-based methods significantly perform better than our method on NIASL2021. This is likely because glosses enhance the alignment of sign pose sequence features with specific linguistic entities, leading to more accurate segmentation and recognition of named entities. Tab. 1 reveals that the higher incidence of named entity in NIASL2021 likely contributes to the better performance of gloss-based methods on this dataset. Moreover, to see how glosses assist and improve model performance, we visualize the attention map in three different SLT models (Joint-SLT with and without gloss supervision, and UniGloR-SLT) in Fig. 3. The visualization result shows that glosses enhance focus on key local areas; ours, even without glosses, shows a similar focus. In SLP, as shown in Tab. 3b, our method outperformed gloss-based methods, showing its robustness and effectiveness in SLP.

## 5.5 Qualitative Results

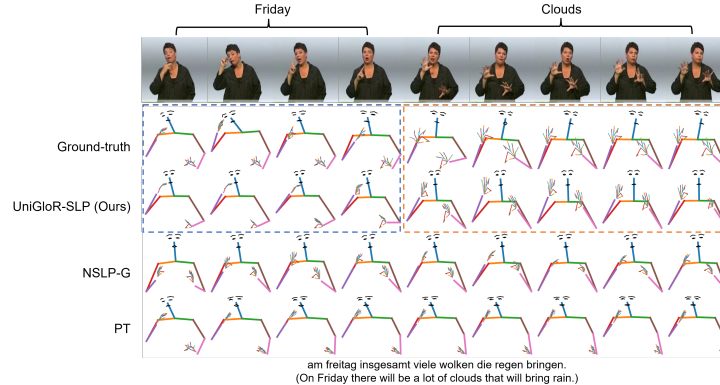
Fig. 4 presents translation and production results of our method and baselines on PHOENIX14T. In the translation results (Fig. 4a), our method accurately translates while others fail to interpret the original meanings. In the production

---

Ground Truth:	und nun die wettervorhersage für morgen donnerstag den sechszwanzigsten november. (And now the weather forecast for tomorrow, Thursday the twenty-sixth of November.)
Joint-SLT <sup>†*</sup> [5]:	und nun die wettervorhersage für morgen samstag den fünfundzwanzigsten dezember. (And now the weather forecast for tomorrow, Saturday the twenty-fifth of December.)
ConSLT* [16]:	und nun die wettervorhersage für morgen freitag den siebenundzwanzigsten mai. (And now the weather forecast for tomorrow, Friday the twenty-seventh of May.)
Ours:	und nun die wettervorhersage für morgen donnerstag den sechszwanzigsten november. (And now the weather forecast for tomorrow, Thursday the twenty-sixth of November.)

---

(a) Comparison of example translation results from ours and previous SLT methods, with correctly translated 1-grams highlighted in blue.



(b) Visualization of the production results with uniformly selected frames, where our method yield better quality through more accurate sign poses. The blue and orange dashed box shows better representation of “friday” and “cloud”, respectively.

**Fig. 4:** (a) Translation and (b) production results on PHOENIX14T. More results can be found in the supplementary material.

results (Fig. 4b), our method generates more accurate sign poses. More results can be found in the supplementary material. Furthermore, we present a visualization of the learned embedding space of UniGloR on NIASL2021, as shown in Fig. 5a. NIASL2021 is the only dataset providing gloss-level annotation for sign language analysis. The result shows distinct clusters, indicating that UniGloR successfully learns meaningful and discriminative features, essential for accurate translation and production.

## 5.6 Ablation and Additional Experiments

We investigated the effects of different components and design choices of our method on PHOENIX14T, which is the most widely used in sign language research. First, we evaluated the impact of APW on our methods, as well as on prior SLT and SLP methods. We established three different scenarios: one without weighting ( $W = \mathbf{1}$ ), one with Fixed Pose Weights (FPW) using static weights for all the training samples, and one with APW. For FPW, we used weights of 1.0, 1.17, and 1.18 for the body, face, and hands, respectively, which were derived from the entire dataset statistics. Tab. 4 demonstrates that integrating APW enhances performance across all methods, indicating that its dynamic emphasis on informative pose segments leads to a more refined representation and hence improves the translation and production performance.

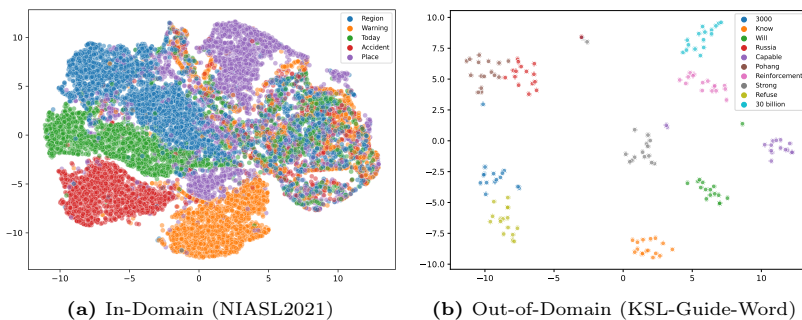


**Fig. 5:** Visualization of learned UniGloR spaces on NIASL2021 and KSL-Guide-Word. We selected five and ten frequent glosses, respectively. T-SNE [41] was used for the 2D plot; each point corresponds to a UniGloR feature from a gloss-level sign segment.

**Table 4:** An analysis of the effects of APW and FPW on SLT and SLP methods on PHOENIX14T. For FPW, weights were manually extracted from the dataset.

Models	B@1	B@2	B@3	B@4	R@L	Models	B@1	B@2	B@3	B@4	R@L	MPJPE↓
UniGloR-SLT	24.73	16.51	12.25	9.80	24.75	UniGloR-SLP	25.03	17.59	13.71	11.23	26.95	0.211
+ FPW	24.96	16.94	12.70	10.24	24.93	+ FPW	27.62	19.64	15.12	12.34	29.64	0.191
+ APW	<b>26.68</b>	<b>18.22</b>	<b>13.73</b>	<b>11.01</b>	<b>27.03</b>	+ APW	<b>29.60</b>	<b>21.25</b>	<b>16.48</b>	<b>13.44</b>	<b>31.38</b>	<b>0.183</b>
Joint-SLT <sup>†</sup> * [5]	21.31	14.17	10.05	8.12	22.56	PT <sup>‡</sup> [51]	12.07	5.94	4.04	3.08	11.06	0.602
+ FPW	23.45	15.16	10.95	8.52	22.78	+ FPW	13.45	6.88	4.65	3.47	12.03	0.579
+ APW	<b>24.22</b>	<b>15.92</b>	<b>11.61</b>	<b>9.11</b>	<b>23.47</b>	+ APW	<b>13.52</b>	<b>7.12</b>	<b>5.03</b>	<b>3.99</b>	<b>12.14</b>	<b>0.559</b>
ConSLT* [16]	21.09	13.93	10.48	8.49	21.81	NSLP-G [23]	19.10	12.10	8.87	6.97	18.62	0.335
+ FPW	21.16	14.09	10.53	8.50	21.50	+ FPW	18.98	12.15	8.87	6.96	18.47	0.336
+ APW	<b>22.16</b>	<b>14.91</b>	<b>11.15</b>	<b>9.00</b>	<b>22.18</b>	+ APW	<b>19.80</b>	<b>12.56</b>	<b>9.06</b>	<b>7.11</b>	<b>19.37</b>	<b>0.333</b>

(a) Translation performance

(b) Production performance

Then, we explored how various components, including decoding, pooling, window size, and dataset composition, impact the downstream SLT. We found that non-autoregressive decoding marginally outperforms autoregressive decoding, suggesting that autoregression might not be essential (Tab. 5a). We observed similar effectiveness between mean and CLS pooling, indicating that the choice of pooling might not be critical (Tab. 5b). Increasing the window size appeared to reduce the focus on key features, supporting our choice based on [63] (Tab. 5c). Varied training data, in terms of dataset sampling ratio and scale, highlighted the importance of diversity in training data (Tab. 5d).

Lastly, we extended our application to Sign Language Recognition (SLR), evaluating its adaptability. As shown in Tab. 5e, our method outperformed the existing SLR methods by a significant margin in Top-1 accuracy. Moreover, Fig. 5b demonstrates UniGloR’s effectiveness in clustering, showing its capability to extract accurate and meaningful representations from out-of-domain data in a zero-shot manner. This indicates the broad application scope of UniGloR, confirming its effectiveness across sign language tasks.

## 5.7 Limitations and Discussion

Although UniGloR has shown promising results in SLT, SLP, and SLR, we acknowledge several limitations in our method. Our method relies on extracted

**Table 5:** Ablation experiments on PHOENIX14T. P, H, and N denote PHOENIX14T, How2Sign, and NIASL2021, respectively. We also report the recognition results on KSL-Guide-Word dataset [18].

Decoding Type			Pooling Type			Window Size		
Decoding Type	B@4	R@L	Pooling Type	B@4	R@L	Window Size	B@4	R@L
AR	10.42	26.66	Mean	<b>11.12</b>	<b>27.47</b>	N=32	8.59	23.10
NAR (ours)	<b>11.01</b>	<b>27.03</b>	CLS (ours)	11.01	27.03	N=64	8.15	22.32
(a) Decoding Type			(b) Pooling Type			(c) Window Size		

Dataset(Proportion Used)			SLR Models			
Dataset(Proportion Used)	B@4	R@L	SLR Models	Top-1	Top-5	Top-10
PHOENIX14T	9.10	23.31	GRU + Normalization [27]	90.46	-	-
PHOENIX14T+How2Sign(10%)+NIASL2021(2%)	9.29	23.66	Multi Transformer Encoder [48]	91.01	-	-
PHOENIX14T+How2Sign	10.41	25.95	UniGloR-SLR (Ours)	<b>95.03</b>	<b>97.82</b>	<b>98.00</b>
PHOENIX14T+How2Sign+NIASL2021(10%)	10.66	25.93				
PHOENIX14T+How2Sign+NIASL2021	<b>11.01</b>	<b>27.03</b>				
(d) Dataset Composition			(e) Recognition Performance			

keypoints from sign language videos to reduce the high computational cost associated with processing RGB modalities. This keypoint-based approach, while offering universal applicability, might result in some loss of detail, potentially leading to lower performance in SLT compared to methods that utilize full RGB data [32, 37, 65]. This compromise was a necessary trade-off for computational efficiency. UniGloR can be also pre-trained on recently available large-scale datasets such as BOBSL [1] and Youtube-ASL [59]. However, our focus was on diverse datasets in low-resource settings, though we plan to explore the large-scale datasets for self-supervised learning. In SLP, due to the lack of high-fidelity character representation such as SMPL-X [45], the generated outputs may not look convincing. However, our main focus was on the accuracy of SLP, which was evaluated with back-translation. Future work could aim at enhancing the realism of sign poses by using high-fidelity characters or generating videos.

Our method learns from randomly segmented sign language motions, significantly reducing the computational overhead, even when considering the integration with RGB modality, compared to using full sequence of sign language. Therefore, as a future work, we plan to extend UniGloR with RGB modality with Masked Autoencoders (MAE) [15, 58] for the gloss-free approach. This enables downstream models to further reduce computational demands while improving the ability to process and interpret sign language more effectively and efficiently.

## 6 Conclusion

In this paper, we introduce UniGloR, a novel and comprehensive solution for both SLT and SLP, utilizing a self-supervised learning approach to understand complex spatio-temporal dynamics of sign language. We improve UniGloR’s applicability by eliminating the need for external annotation and fine-tuning. Moreover, we introduce APW to capture subtle yet critical features, such as facial expressions and hand movements, pivotal in sign language. The extensive experiments have demonstrated that our method outperforms existing SLT and SLP, and SLR methods and reduces the reliance on the traditionally used resource-intensive gloss annotations.

## References

1. Albanie, S., Varol, G., Momeni, L., Bull, H., Afouras, T., Chowdhury, H., Fox, N., Woll, B., Cooper, R., McParland, A., Zisserman, A.: BOBSL: BBC-Oxford British Sign Language Dataset (2021) [14](#)
2. Cai, L., Song, Y., Liu, T., Zhang, K.: A hybrid bert model that incorporates label semantics via adjustive attention for multi-label text classification. *IEEE Access* **8**, 152183–152192 (2020) [8](#)
3. Cai, Y., Huang, L., Wang, Y., Cham, T., Cai, J., Yuan, J., Liu, J., Yang, X., Zhu, Y., Shen, X., Liu, D., Liu, J., Magnenat-Thalmann, N.: Learning progressive joint propagation for human motion prediction. In: *ECCV*. pp. 226–242 (2020) [9](#)
4. Camgöz, N.C., Hadfield, S., Koller, O., Ney, H., Bowden, R.: Neural sign language translation. In: *CVPR*. pp. 7784–7793 (2018) [3](#), [8](#), [9](#)
5. Camgöz, N.C., Koller, O., Hadfield, S., Bowden, R.: Sign language transformers: Joint end-to-end sign language recognition and translation. In: *CVPR*. pp. 10020–10030 (2020) [1](#), [3](#), [4](#), [9](#), [10](#), [12](#), [13](#)
6. Cao, Z., Hidalgo, G., Simon, T., Wei, S.E., Sheikh, Y.: Openpose: Realtime multi-person 2d pose estimation using part affinity fields. *IEEE Trans. Pattern Anal. Mach. Intell.* **43**(1), 172–186 (jan 2021) [8](#)
7. Chen, Y., Zuo, R., Wei, F., Wu, Y., Liu, S., Mak, B.: Two-stream network for sign language recognition and translation. In: *NeurIPS*. vol. 35, pp. 17043–17056 (2022) [4](#)
8. Chen, Y., Zhang, Z., Yuan, C., Li, B., Deng, Y., Hu, W.: Channel-wise topology refinement graph convolution for skeleton-based action recognition. In: *ICCV*. pp. 13339–13348 (2021) [5](#), [9](#), [10](#)
9. Cheng, Y., Wei, F., Bao, J., Chen, D., Zhang, W.: Cico: Domain-aware sign language retrieval via cross-lingual contrastive learning. In: *CVPR*. pp. 19016–19026 (2023) [2](#), [3](#)
10. Devlin, J., Chang, M., Lee, K., Toutanova, K.: BERT: pre-training of deep bidirectional transformers for language understanding. In: *Conference of the North American Chapter of the Association for Computational Linguistics*. pp. 4171–4186 (2019) [5](#)
11. Dirting, B.D., Chukwudebe, G.A., Nwokorie, E.C., Ayogu, I.I.: Multi-label classification of hate speech severity on social media using bert model. In: *NIGERCON*. pp. 1–5. *IEEE* (2022) [8](#)
12. Dosovitskiy, A., Beyer, L., Kolesnikov, A., Weissenborn, D., Zhai, X., Unterthiner, T., Dehghani, M., Minderer, M., Heigold, G., Gelly, S., Uszkoreit, J., Houshy, N.: An image is worth 16x16 words: Transformers for image recognition at scale. In: *ICLR* (2021) [5](#)
13. Duarte, A.C., Albanie, S., Giró-i-Nieto, X., Varol, G.: Sign language video retrieval with free-form textual queries. In: *CVPR*. pp. 14074–14084 (2022) [2](#), [3](#)
14. Duarte, A.C., Palaskar, S., Ventura, L., Ghadiyaram, D., DeHaan, K., Metze, F., Torres, J., Giró-i-Nieto, X.: How2sign: A large-scale multimodal dataset for continuous american sign language. In: *CVPR*. pp. 2735–2744 (2021) [3](#), [8](#), [9](#)
15. Feichtenhofer, C., Li, Y., He, K., et al.: Masked autoencoders as spatiotemporal learners. In: *NeurIPS*. vol. 35, pp. 35946–35958 (2022) [14](#)
16. Fu, B., Ye, P., Zhang, L., Yu, P., Hu, C., Shi, X., Chen, Y.: A token-level contrastive framework for sign language translation. In: *ICASSP*. pp. 1–5 (2023) [3](#), [9](#), [10](#), [12](#), [13](#)

17. Guo, W., Du, Y., Shen, X., Lepetit, V., Alameda-Pineda, X., Moreno-Noguer, F.: Back to MLP: A simple baseline for human motion prediction. In: *IEEE/CVF WACV*. pp. 4798–4808 (2023) [9](#)
18. Ham, S., Park, K., Jang, Y., Oh, Y., Yun, S., Yoon, S., Kim, C.J., Park, H., Kweon, I.S.: Ksl-guide: A large-scale korean sign language dataset including interrogative sentences for guiding the deaf and hard-of-hearing. In: *IEEE FG*. pp. 1–8 (2021) [2](#), [3](#), [8](#), [14](#)
19. Hao, A., Min, Y., Chen, X.: Self-mutual distillation learning for continuous sign language recognition. In: *ICCV*. pp. 11283–11292 (2021) [4](#)
20. Hu, H., Zhao, W., Zhou, W., Wang, Y., Li, H.: Signbert: Pre-training of hand-model-aware representation for sign language recognition. In: *ICCV*. pp. 11067–11076 (2021) [4](#)
21. Huang, W., Pan, W., Zhao, Z., Tian, Q.: Towards fast and high-quality sign language production. In: *ACM MM*. pp. 3172–3181 (2021) [1](#), [3](#), [6](#), [9](#), [10](#), [11](#)
22. Huerta-Enochian, M., Lee, D.H., Myung, H.J., Byun, K.S., Lee, J.W.: Kosign sign language translation project: Introducing the niasl2021 dataset. In: *International Workshop on Sign Language Translation and Avatar Technology*. pp. 59–66 (2022) [3](#), [8](#), [9](#)
23. Hwang, E.J., Kim, J., Park, J.C.: Non-autoregressive sign language production with gaussian space. In: *BMVC*. p. 197 (2021) [3](#), [6](#), [8](#), [9](#), [10](#), [11](#), [13](#)
24. Hwang, E.J., Lee, H., Park, J.C.: Autoregressive sign language production: A gloss-free approach with discrete representations. *arXiv preprint arXiv:2309.12179* (2023) [9](#), [10](#), [11](#)
25. Jiang, Z., Moryossef, A., Müller, M., Ebling, S.: Machine translation between spoken languages and signed languages represented in signwriting. In: *Findings of the Association for Computational Linguistics: EACL 2023*. pp. 1661–1679 (2023) [3](#)
26. Joze, H.R.V., Koller, O.: MS-ASL: A large-scale data set and benchmark for understanding american sign language. In: *BMVC* (2019) [2](#), [4](#)
27. Kim, J.H., Jung, H.G.: Sign-language word recognition using combination of open-pose and gru. In *Proceedings of the Korean Institute of Electronics Engineers Conference* pp. 520–523 (2022) [14](#)
28. Kim, J., Hwang, E.J., Cho, S., Lee, D.H., Park, J.C.: Sign language production with avatar layering: A critical use case over rare words. In: *Proceedings of the Thirteenth Language Resources and Evaluation Conference*. pp. 1519–1528 (2022) [1](#), [3](#)
29. Koller, O., Camgöz, N.C., Ney, H., Bowden, R.: Weakly supervised learning with multi-stream cnn-lstm-hmms to discover sequential parallelism in sign language videos. *IEEE transactions on pattern analysis and machine intelligence* **42**(9), 2306–2320 (2019) [4](#)
30. Lehečka, J., Švec, J., Ircing, P., Šmídl, L.: Adjusting bert’s pooling layer for large-scale multi-label text classification. In: *International Conference on Text, Speech, and Dialogue*. pp. 214–221. Springer (2020) [8](#)
31. Li, D., Opazo, C.R., Yu, X., Li, H.: Word-level deep sign language recognition from video: A new large-scale dataset and methods comparison. In: *IEEE/CVF WACV*. pp. 1448–1458 (2020) [2](#), [4](#)
32. Li, D., Xu, C., Yu, X., Zhang, K., Swift, B., Suominen, H., Li, H.: Tspnet: Hierarchical feature learning via temporal semantic pyramid for sign language translation. In: *NeurIPS*. vol. 33, pp. 12034–12045 (2020) [2](#), [3](#), [7](#), [14](#)
33. Li, D., Yu, X., Xu, C., Petersson, L., Li, H.: Transferring cross-domain knowledge for video sign language recognition. In: *CVPR*. pp. 6204–6213 (2020) [4](#)



34. Li, J., Li, D., Savarese, S., Hoi, S.C.H.: BLIP-2: bootstrapping language-image pre-training with frozen image encoders and large language models. In: ICML. pp. 19730–19742 (2023) [6](#)
35. Li, M., Chen, S., Zhang, Z., Xie, L., Tian, Q., Zhang, Y.: Skeleton-parted graph scattering networks for 3d human motion prediction. In: ECCV. pp. 18–36. Springer (2022) [9](#)
36. Lin, C., Och, F.J.: Automatic evaluation of machine translation quality using longest common subsequence and skip-bigram statistics. In: ACL. pp. 605–612 (2004) [9](#)
37. Lin, K., Wang, X., Zhu, L., Sun, K., Zhang, B., Yang, Y.: Gloss-free end-to-end sign language translation. In: ACL. pp. 12904–12916 (2023) [2](#), [3](#), [5](#), [14](#)
38. Liu, N., Wang, Q., Ren, J.: Label-embedding bi-directional attentive model for multi-label text classification. *Neural Processing Letters* **53**, 375–389 (2021) [8](#)
39. Liu, Z., Zhang, H., Chen, Z., Wang, Z., Ouyang, W.: Disentangling and unifying graph convolutions for skeleton-based action recognition. In: CVPR. pp. 140–149 (2020) [5](#), [9](#), [10](#)
40. Loshchilov, I., Hutter, F.: Decoupled weight decay regularization. In: ICLR (2019) [9](#)
41. der Maaten, V., Laurens, Hinton, G.: Visualizing data using t-sne. *Journal of machine learning research* **9**(11) (2008) [13](#)
42. Min, Y., Hao, A., Chai, X., Chen, X.: Visual alignment constraint for continuous sign language recognition. In: ICCV. pp. 11522–11531 (2021) [4](#)
43. NC, G., Ladi, M., Negi, S., Selvaraj, P., Kumar, P., Khapra, M.M.: Addressing resource scarcity across sign languages with multilingual pretraining and unified-vocabulary datasets. *Advances in Neural Information Processing Systems* **35**, 36202–36215 (2022) [4](#)
44. Papineni, K., Roukos, S., Ward, T., Zhu, W.: Bleu: a method for automatic evaluation of machine translation. In: ACL. pp. 311–318 (2002) [9](#)
45. Pavlakos, G., Choutas, V., Ghorbani, N., Bolkart, T., Osman, A.A., Tzionas, D., Black, M.J.: Expressive body capture: 3d hands, face, and body from a single image. In: CVPR. pp. 10975–10985 (2019) [14](#)
46. Ramesh, A., Pavlov, M., Goh, G., Gray, S., Voss, C., Radford, A., Chen, M., Sutskever, I.: Zero-shot text-to-image generation. In: ICML. vol. 139, pp. 8821–8831 (2021) [7](#)
47. Rastgoo, R., Kiani, K., Escalera, S., Athitsos, V., Sabokrou, M.: All you need in sign language production. *arXiv preprint arXiv:2201.01609* (2022) [1](#)
48. Roh, K., Hwang, E.J., Lee, H., Park, J.C.: Korean sign language recognition on keypoints with a transformer model. In: Proceedings of the Korean Institute of Electronics Engineers Conference pp. 1074–1076 (2023) [14](#)
49. Sanh, V., Debut, L., Chaumond, J., Wolf, T.: Distilbert, a distilled version of BERT: smaller, faster, cheaper and lighter. *arXiv preprint arXiv:1910.01108* (2019) [5](#), [7](#)
50. Saunders, B., Bowden, R., Camgöz, N.C.: Adversarial training for multi-channel sign language production. In: BMVC (2020) [3](#), [6](#)
51. Saunders, B., Camgöz, N.C., Bowden, R.: Progressive transformers for end-to-end sign language production. In: ECCV. pp. 687–705. Springer (2020) [3](#), [6](#), [8](#), [9](#), [10](#), [11](#), [13](#)
52. Saunders, B., Camgöz, N.C., Bowden, R.: Mixed signals: Sign language production via a mixture of motion primitives. In: ICCV. pp. 1899–1909 (2021) [3](#), [6](#)

53. Saunders, B., Camgöz, N.C., Bowden, R.: Signing at scale: Learning to co-articulate signs for large-scale photo-realistic sign language production. In: CVPR. pp. 5131–5141 (2022) [2](#), [3](#)
54. Shalev-Arkushin, R., Moryossef, A., Fried, O.: Ham2pose: Animating sign language notation into pose sequences. In: CVPR. pp. 21046–21056 (2023) [1](#), [3](#)
55. Shi, B., Brentari, D., Shakhnarovich, G., Livescu, K.: Open-domain sign language translation learned from online video. In: Conference on Empirical Methods in Natural Language Processing. pp. 6365–6379 (2022) [2](#)
56. Stenum, J., Cherry-Allen, K.M., Pyles, C.O., Reetzke, R.D., Vignos, M.F., Roemich, R.T.: Applications of pose estimation in human health and performance across the lifespan. *Sensors* **21**(21), 7315 (2021) [6](#)
57. Tang, S., Hong, R., Guo, D., Wang, M.: Gloss semantic-enhanced network with online back-translation for sign language production. In: ACM MM. pp. 5630–5638 (2022) [1](#), [3](#), [6](#), [9](#), [10](#), [11](#)
58. Tong, Z., Song, Y., Wang, J., Wang, L.: Videomae: Masked autoencoders are data-efficient learners for self-supervised video pre-training. In: NeurIPS. vol. 35, pp. 10078–10093 (2022) [14](#)
59. Uthus, D., Tanzer, G., Georg, M.: Youtube-asl: A large-scale, open-domain american sign language-english parallel corpus. *NeurIPS* **36** (2024) [14](#)
60. Vaswani, A., Shazeer, N., Parmar, N., Uszkoreit, J., Jones, L., Gomez, A.N., Kaiser, L., Polosukhin, I.: Attention is all you need. In: *NeurIPS*. p. 6000–6010. NIPS’17, Curran Associates Inc., Red Hook, NY, USA (2017) [5](#), [9](#)
61. Viegas, C., Inan, M., Quandt, L.C., Alikhani, M.: Including facial expressions in contextual embeddings for sign language generation. In: Joint Conference on Lexical and Computational Semantics. pp. 1–10 (2023) [1](#), [3](#)
62. Voskou, A., Panousis, K.P., Kosmopoulos, D.I., Metaxas, D.N., Chatzis, S.: Stochastic transformer networks with linear competing units: Application to end-to-end SL translation. In: ICCV. pp. 11926–11935 (2021) [2](#)
63. Wilbur, R.B.: Effects of varying rate of signing on asl manual signs and nonmanual markers. *Language and speech* **52**(2-3), 245–285 (2009) [9](#), [13](#)
64. Yin, A., Zhao, Z., Liu, J., Jin, W., Zhang, M., Zeng, X., He, X.: Simulslt: End-to-end simultaneous sign language translation. In: ACM MM. pp. 4118–4127 (2021) [1](#), [3](#)
65. Yin, A., Zhong, T., Tang, L., Jin, W., Jin, T., Zhao, Z.: Gloss attention for gloss-free sign language translation. In: CVPR. pp. 2551–2562 (2023) [2](#), [4](#), [14](#)
66. Zelinka, J., Kanis, J.: Neural sign language synthesis: Words are our glosses. In: IEEE/CVF WACV. pp. 3395–3403 (2020) [8](#)
67. Zhang, B., Müller, M., Sennrich, R.: SLTUNET: A simple unified model for sign language translation. In: ICLR (2023) [3](#), [10](#)
68. Zhang, H., Guo, Z., Yang, Y., Liu, X., Hu, D.: C2st: Cross-modal contextualized sequence transduction for continuous sign language recognition. In: ICCV. pp. 21053–21062 (2023) [4](#)
69. Zhou, H., Zhou, W., Qi, W., Pu, J., Li, H.: Improving sign language translation with monolingual data by sign back-translation. In: CVPR. pp. 1316–1325 (2021) [1](#), [3](#)
70. Zhou, H., Zhou, W., Zhou, Y., Li, H.: Spatial-temporal multi-cue network for sign language recognition and translation. *IEEE TMM* **24**, 768–779 (2022) [1](#), [3](#), [4](#)
71. Zhou, Y., Wang, Z., Fang, C., Bui, T., Berg, T.L.: Dance dance generation: Motion transfer for internet videos. In: ICCVW. pp. 1208–1216 (2019) [6](#)
72. Zuo, R., Wei, F., Mak, B.: Natural language-assisted sign language recognition. In: CVPR. pp. 14890–14900 (2023) [4](#)